JOURNAL OF MATERIALS SCIENCE 19 (1984) 1997–2012

Stress–orientation–strain relationships in non-crystalline polymers

Part 1 *Strategy for a model*

D. J. BROWN, A. H. WINDLE
Department of Metallurgy and Materials Science, University of Cambridge, Cambridge, UK

This paper, the first in a series of three, outlines a novel approach to the description of polymer deformation in both rubbery and glassy states. The ability of affine models to predict stress–orientation–strain (SOS) relationships across a range of polymers in the rubbery regime is first reviewed, together with the application of the pseudo-affine model to the orientation–strain behaviour of plastically deformed glasses. An alternative strategy is then introduced, in which deformation of rubber or glass is resolved into an orientational component (associated with the alignment of individual chain units) and an extensional component (associated with the "unravelling" of the macromolecular chain). Both molecular orientation and overall strain are seen as aspects of the system's response to stress, but the relationship between them is not unique, being dependent on temperature and the nature of the units making up the chain segments.

1. Introduction

The deformation of materials can be studied either on a macroscopic or on a microscopic scale. The macroscopic approach is best exemplified by the familiar stress–strain test; the microscopic approach will concern local deformation processes on (at least initially) the scale of a few atoms or molecules. Stress–strain behaviour alone does not offer a complete characterization of the deformation behaviour of a non-crystalline polymer, either above or below the glass transition. However, one principal consequence of deformation will be the creation of some degree of alignment among molecular segments: such aligment can be quantified in terms of spherical harmonic parameters and it will lead to anisotropy of properties. By attempting to measure the degree of molecular alignment as a function of stress or strain, one may obtain information about deformation processes on a microscopic scale. A comprehensive view of polymer deformation would encompass both mechanical (stress–strain) and orientation–strain behaviour, and would be applicable to polymers of differing molecular structure. Additionally, such a view should provide a framework for the description of deformation behaviour over a range of temperature above and below T_g.

This series of papers presents a first step towards such a unified view. In this paper (Part 1) we firstly survey the broad spectrum of knowledge concerning the orientational behaviour of non-crystalline polymers in relation to mechanical behaviour, and identify several features which call into question the common assumption of a direct relationship between molecular orientation and strain. Secondly, we put forward an approach to polymer deformation above the glass transition which will, potentially, allow description of both mechanical and orientation behaviour. The proposed strategy involves the resolution of deformation into orientational and non-orientation components.

In Part 2, we employ this approach as the basis of a simple deformation model, allowing quantitative description, at least to a first approximation, of deformation processes; and in Part 3, we relate the "rubber-like" behaviour to plastic deformation below T_g, where strain rate (or in effect, time) becomes an important factor.

0022–2461/84 $03.00 + .12

2. The outstanding questions

2.1. The emphasis of established theories

An early success of polymer science was the description, in the 1940s, of the characteristic stress–strain curve of natural rubber (*cis*-polyisoprene). Starting from the basic assumptions of a molecular network and that the deformation of the network points is affine (i.e. the points behave as though they were embedded in an elastic continuum), the entropy-driven elasticity of the material was modelled by the Gaussian statistical theory in terms of a single parameter equivalent to the number N of macromolecular chain segments per unit volume. Further refinement within the framework of the so-called affine scheme of deformation involved the introduction of a second parameter n, the effective number of statistical links per chain, and predicted a maximum extension ratio for the rubber network, $\lambda_{max} = n^{1/2}$, though at the cost of increased mathematical complexity.

The affine statistical theory also proved useful in the analysis of the well-known phenomenon of rubbery photoelasticity, in which the preferential alignment of chain segments gives rise to increasing optical birefringence (see Appendix).

The foundations of rubber elasticity theory were therefore established prior to the post-war development of a wide range of synthetic high polymers. Many of these display rubbery mechanical behaviour which is qualitatively similar to *cis*-polyisoprene, although not necessarily in the same temperature range. In fact, some of these materials appear more amenable to analysis than natural rubber, by virtue of being better characterized (through their non-biological origin) and less susceptible to the complicating and contenious problem of strain-induced crystallization. Nevertheless, in the continuing theoretical development of rubber elasticity, experimental comparisons have been made using data almost exclusively from natural rubber and its close relatives.

In addition to the increasing availability of different polymers which behave as rubbers at an appropriate temperature, there has been the development of new methods for determining molecular orientation. Details of the techniques are given elsewhere [1–5], and the formalism by which orientation may be quantified in terms of a series of spherical harmonic parameters, rather like the Fourier components of a waveform, is summarized in the Appendix.

*See Appendix for definitions.

Theoretical predictions of the development of orientation with strain have traditionally been tested against birefringence data. For this reason it is useful to underline the limitations of this measurement of orientation when used alone:

(i) it yields only the first term in the spherical harmonic series (birefringence $\propto \langle P_2(\cos\phi)\rangle^*$); other techniques can yield more, with wide angle X-ray scattering able, at least in principle, to give any term in the series.

(ii) it yields only a relative measure of $\langle P_2(\cos\phi)\rangle$, since an accurate value for the birefringence which would correspond to complete molecular orientation (the intrinsic birefringence) is both experimentally and theoretically inaccessible.

(iii) it is difficult to separate the measured birefringence into the component due to orientation of the molecular chains, and the component (significant at high stresses) resulting from elastic distortion of both the local conformation and the chain packing by the applied stress. This latter component is referred to as "elastic birefringence" and corresponds to the pre-yield birefringence seen in polymer glasses which is not associated with chain orientation [6].

It is thus important, when endeavouring to analyse orientation behaviour, to take a broader view than that afforded by photoelasticity *per se*.

2.2. Predictions of affine and pseudo-affine schemes

Fig. 1 shows stress–strain data for natural rubber, fitted by one of the affine but non-Gaussian models for rubber elasticity. An "n" of 75 links per chains segment has to be assumed if the observed maximum strain is to be equal to $n^{1/2}$ as the elementary theory requires. The value of the "rubber modulus", NkT, is chosen to give the best fit at intermediate to high strains, though this gives rather too low an initial slope and neglects the influence of crystallization at high strains.

The birefringence–strain plot for natural rubber (Fig. 2) exhibits the pronounced curvature predicted by affine models. Quantitative comparison with the affine prediction for $\langle P_2\rangle$ against strain is difficult, however, since a value for intrinsic birefringence $\Delta\mu_0$ (corresponding to $\langle P_2\rangle = 1$) must be estimated. The Gaussian form of the affine scheme predicts that at the limiting strain of $\lambda = n^{1/2}$, the birefringence $\Delta\mu$ should be given by:

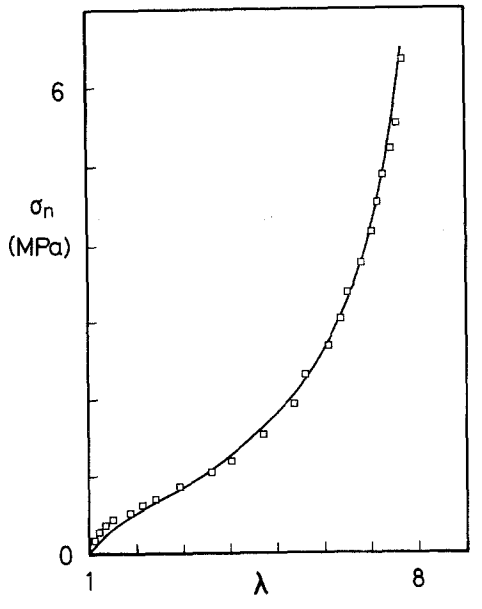

Figure 1 Nominal stress–strain curve for the James–Guth 3-chain affine model, fitted to experimental data of Treloar [7] (□), after Treloar [8]. The parameters $n = 75$, $NkT = 0.273$ MPa have been chosen to fit the data at high strains: this results in a rather poor fit for $\lambda \lesssim 3$.

$$\frac{\Delta\mu}{\Delta\mu_0} = \langle P_2 \rangle = \frac{1}{5n}(n - 1/n^{1/2})$$

$$\simeq 0.2 \qquad \text{for large } n.$$

This limit of 0.2 is greatly increased if a non-Gaussian model is chosen, so that estimation of $\Delta\mu_0$ by extrapolation is impracticable, while calculated values such as Treloar's 0.28 [9] involve rather severe approximations. The choice of a smaller $\Delta\mu_0$ implies that a smaller n is required to fit the data, and Treloar himself uses the case $n = 25$ for comparison of the various theoretical affine models available [8]. The predicted $\langle P_2 \rangle$ against λ curves for such models are dependent solely on n.

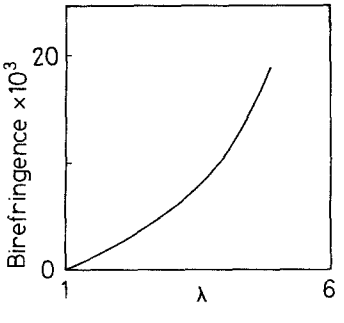

Figure 2 Birefringence against extension ratio for natural rubber at 25° C, after Treloar [9].

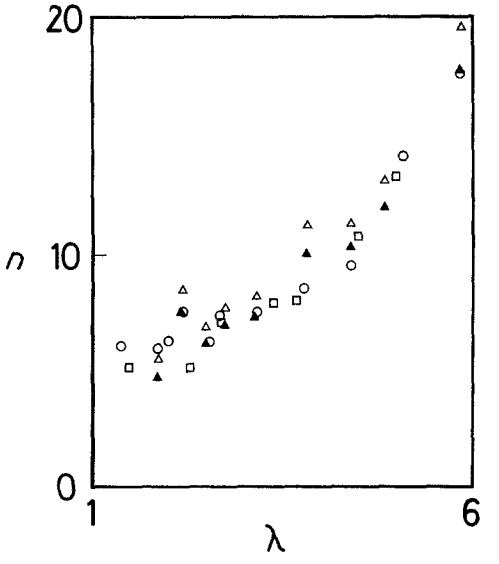

Figure 3 Number of links per affine chain, n, against strain for PET drawn at 80° C: ▲ Purvis and Bower [10] (laser-Raman spectroscopy, 1616 cm^{-1} line), conformational model "A"; △ *ibid.*, conformational model "B"; □ Cunningham, Ward, Willis and Zichy [11] (i.r. spectroscopy); ○ Nobbs, Bower, Ward and Patterson [12] (polarized fluorescence, assuming "model 1" for the optical behaviour of the fluorescent molecule and converting to $\langle P_2 \rangle$ for the PET by means of Fig. 1 of Nobbs *et al.* [13]).

Some uncertainty is indicated, then, in reconciling the mechanical and the orientational predictions of the affine deformation scheme, and the difficulty is highlighted by studies of polymers better characterized than natural rubber. These have the advantage that absolute values of $\langle P_2 \rangle$, rather than simply birefringence measurements, are available. Such data, when plotted as an orientation–strain curve, show less evidence of the upward curvature characteristic of natural rubber: the affine scheme can consequently fit the data only if n is permitted to vary with strain. As an example, Fig. 3 shows the required variation of n for PET and Fig. 4 a similar plot for PMMA. We note that at low strains the necessary n is small.

In the case of the PMMA data (Fig. 4), the value of n at zero strain is close to one, which prompts consideration of a situation where there is only one link per chain, so that molecular segments essentially orient as rigid rods. Such behaviour would be accompanied by a very rapid development of orientation as measured by $\langle P_2 \rangle$ (similar to that seen in polymer glasses at low strains). It can be described by the pseudo-affine deformation scheme [16] first introduced by Kratky [17] in connection with the orientation of crystallites in a

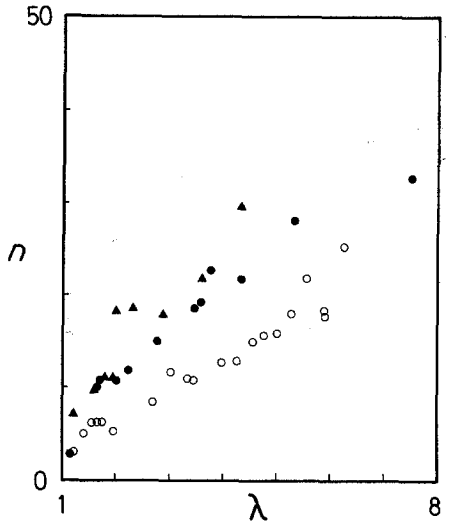

Figure 4 "n" against strain for PMMA from WAXS data. T_g is approximately 105° C. ○ 125° C, plane strain compression (Pick *et al.* [6]); • 150° C, plane strain compression (Pick *et al.* [6]); ▲ 150° C, uniaxial tension (Brown and Mitchell [14]). The measured strains at 150° C will include some element of irrecoverable plastic flow. This amounted to some 12% of true strain at $\lambda = 4.3$ [15].

non-crystalline matrix. The scheme considers an aggregate of transversely isotropic, rod-like units embedded in a continuum, and the axes of these units are assumed to rotate on deformation in the same manner as lines joining pairs of points in a body which (on the scale of the rods) is deforming affinely (easily visualized as rigid needles in an affinely deforming haystack).

Some success has been achieved by the pseudo-affine scheme in describing the shape, if not the scale, of the $\langle P_2 \rangle$ against strain curve for polymer glasses [1, 2, 16, 18]. However, like the affine scheme of which it is, in essence, a special case, it is limited by the assumption of a unique relationship between orientation and strain, so that no further advance is afforded in interpreting the temperature dependence of the experimental orientation–strain relationship, or differences in the annealing and recovery behaviour of orientation and strain. Indeed, it in a sense leaves one worse off, since one can no longer argue in terms of a temperature-dependent n as has been possible in the affine case [19, 20], for n has been fixed, for better or for worse, at 1.

2.3. The influence of temperature

Despite the paucity of data, it seems clear that there is a very considerable temperature dependence of the orientation–strain plot. The slope of the $\langle P_2 \rangle$–strain curve increases rapidly with falling temperature, with a gradual transition to the decelerating $\langle P_2 \rangle$–strain curve characteristic of the glassy state (Fig. 5).

The statistical theory for rubber does not directly predict any such temperature dependence: it implies that orientation is solely a function of strain. The observed variation has therefore to be interpreted in terms of changes with temperature of the effective size of the "statistical random link", and hence of the number of links per chain. However, as is exemplified by Figs. 3 and 4, the required n would have to be rapidly varying and, near the glass transition, very small indeed at low strains.

2.4. Annealing and stress relaxation

Information about orientation-deformation relationships can be provided by annealing. Brady and Yeh [22] annealed cold-drawn PC below T_g for several days, and a series of flat-plate X-ray photographs showed a loss of most, if not all, of the equatorial arcing indicative of orientation. However, only 28% dimensional recovery occurred; the remaining 72% recovery was not achieved until the sample was reheated above T_g. Similar results [23] were obtained for atactic PS and PMMA. The PS displayed recovery of 27%, and the PMMA 22.5%, of the cold-drawn deformation. Again, complete loss of the X-ray orientation is claimed, although a series of flat-plate photographs is hardly the most precise measure of this parameter. Birefringence was measured for PS only; it recovered below T_g to the extent of 57%.

Brady and Yeh use these observations to support Yeh's proposed structural model for glasses, consisting of "ordered domains" separated by regions of more random chain configuration. The partial strain recovery is attributed to short-range reorganization in the latter region without the longer-range reorganization necessary for domain motion. Without judging this theory, we can at least infer that there appear to be two components to the deformation behaviour, one of which is associated particularly with molecular orientation, and is more readily able to undergo recovery.

Kahar *et al.* [20] also annealed PMMA, oriented by hydrostatic extrusion in the glassy state, at temperatures between the deformation temperature T_d and T_g. Partial strain recovery was observed:

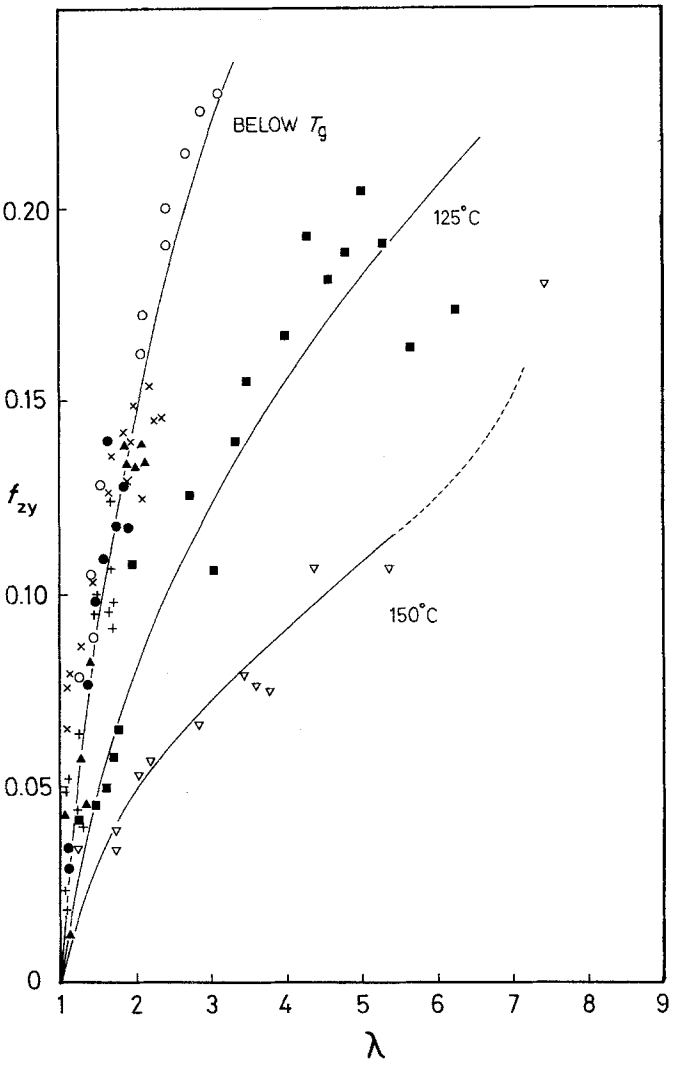

Figure 5 The development of molecular orientation during the plane strain compression of PMMA at different temperatures: + 20° C; • 40° C; ▲ 60° C; × 80° C; ○ 100° C; ■ 125° C; ▽ 150° C. The parameter f_{zy} is closely related to $\langle P_2(\cos\phi)\rangle$. (after Windle A.H., in Ward [21]).

even at 105° C, often taken as T_g for PMMA, only 70% recovery was observed after some 2 days.

Upon annealing above T_g, complete recovery of strain and birefringence occurred. Birefringence at first recovered more rapidly than strain (Fig. 6), which again indicates that an orientation-related component of deformation is more susceptible to recovery than the remaining deformation.

If annealing is carried out at constant length, the shrinkage force can be measured: Kahar *et al.* found that the force decayed from an initial peak to a finite limit with time. Two comparisons were made:

(a) same strain, different T_d and hence birefringence: the more birefringent specimen gave a higher peak force, but the limiting force was unchanged.

(b) same birefringence, different T_d and hence

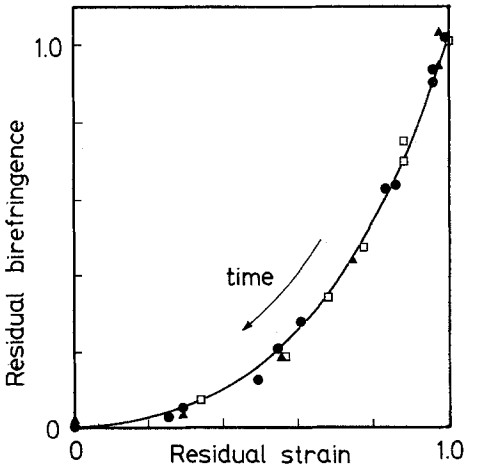

Figure 6 Recovery of PMMA on annealing at 116.5° C, after Kahar *et al.* [20]. Residual birefringence and strain are expressed as fractions of the as-deformed values. T_d = deformation temperature. • T_d = 50° C; ▲ T_d = 90° C; □ T_d = 100° C.

strain; the peak was unchanged, but the greater strain led to a higher limiting shrinkage force.

Kahar *et al.* interpret the finite limiting force in terms of a permanent entanglement network. However, whatever the detailed conclusions, their results again suggest the association of orientation with a particular component of deformation.

Somewhat similar shrinkage force measurements have been performed on PET [13, 24, 25]. While these may be viewed similarly to those for PMMA, the intrusion of crystallization makes the behaviour considerably more complex.

2.5. Stress, orientation and strain

The phenomena examined so far suggest that neither the affine nor the pseudo-affine deformation scheme is fully adequate to describe the interplay between stress, strain and orientation, if a broad spectrum of chemically or mechanically cross-linked polymers is to be considered. The unique relationship between orientation and strain implied by both schemes is called into question by experiment, while $\langle P_2 \rangle$–strain data can be described by the affine scheme only by assuming that the equivalent random chain varies in a manner difficult to reconcile either with stress–strain experiments or with the fundamentally statistical nature of the theory.

Of course, the affine model traditionally finds support from natural rubber data, some of which are very well established indeed. However the support is stronger regarding the stress–strain than the orientation–strain relationship: the particular difficulties associated with the use of birefringence as a measure of orientation have been discussed above.

3. The need for an alternative approach

If a view of deformation is to be developed which has the potential to deal in general terms with the interrelation of the three parameters – in other words, to describe stress–orientation–strain relationships – then one must re-examine some assumptions of the established theories, and adopt a somewhat less restrictive basis than the unique strain–orientation connection which is implicit in the affine and pseudo-affine schemes. To be comprehensive, such a view will on the one hand have to encompass both mechanical (stress–strain) and orientational aspects of deformation, without making the assumption of an automatic and unique connection between orientation and strain. On the other hand, it should also shed some light on the changes in behaviour which become apparent as we move towards and through the glass transition – changes with which the affine approach to rubbery deformation is not able to deal.

With these aims in mind, it is proposed to adopt a strategy which views both overall strain and molecular orientation as aspects of a polymer system's response to the stress field imposed upon it. We think in terms of a small section of the macromolecular chain – small enough to be taken as a rigid unit – and consider the effect, in terms both of orientation of the unit and of consequent strain, of the applied stress acting through the unit's immediate environment (including, of course, forces transmitted along its own chain). By this approach we relate the behaviour of an individual molecular unit directly to the applied stress: we thus link stress and orientation, without using macroscopic strain as an intermediary. A model based upon this idea will then be distinctive in taking stress, rather than strain, as the primary variable for the analysis of deformation.

4. A two-component strategy

As an alternative basis for the description of deformation, it is proposed to adopt a strategy based on the resolution of deformation into an orientational and a non-orientational (or extensional) component.

There are several reasons for adopting this approach. The first is the very different nature of the orientation–strain plots in the rubbery and glassy states. A difference in orientation–stress behaviour might be explained in terms of a single deformation process, subject to stress–driven thermal activation and requiring a greater "driving force" at lower temperatures. The different nature of the orientation–strain plot, however, compels one to consider a situation more complex than a single process responsible for both orientation and strain.

The second reason is the annealing and recovery work discussed above. This requires one to "decouple" orientation from strain to some degree, and to conclude that molecular orientation is more readily susceptible to recovery near to T_g than is overall strain.

The third reason arises from recent interest in the achievement of very high chain extensions. This has been associated with work on extensional

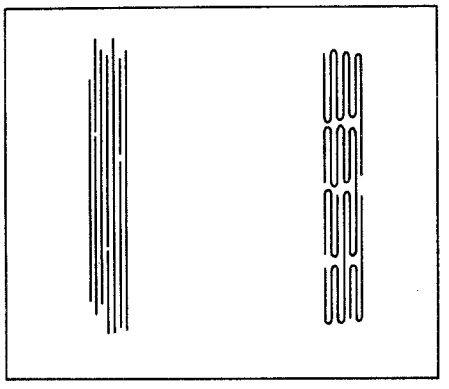

Figure 7 Systems displaying complete chain orientation: (a) fully extended chains, (b) chain folded crystallites.

flow, crystallization from oriented melts or solutions, and the production of high modulus fibres (see the reviews of Keller [26] and of Ciferri and Ward [27]). It has become clear that the achievement of certain properties requires chain extension *per se*, quite apart from chain alignment. This is particularly true of very high elastic moduli, where extension is necessary in order to obtain a high degree of chain continuity along the axis direction [28]. Fig. 7 illustrates the point schematically. The two systems shown both display, in effect, complete orientation (all $\langle P_{2n} \rangle = 1$), but their mechanical properties will be radically different: for example (a), comprising fully extended chains, will have a much greater elastic modulus in the chain direction than (b), which can be regarded as a fibre composed of chain-folded crystallites.

The idea of separating out an orientational component of deformation, with its associated orientation distribution function, is closely related to the proposal of Dobson and Gordon [41] that chain segments containing only one or two bonds should be regarded as "orientationally active" with end-to-end vectors capable of changes in direction but not in magnitude. A comparison may be made with the mathematical formalism proposed by Hsiao and Moghe [29]. However, they do not apply this approach to any specific deformation model, or to the orientational behaviour of real polymers.

We consider, then, the effect of an applied stress field on an assemblage of anisotropic units. We may envisage two ways in which the units can allow the stress to do work, with a consequent macroscopic strain. They may undergo rotation, leading to a preferential unit orientation, but with no change in the disposition of nearest neighbours around a given unit; or they may respond by a bodily shift of their centres of gravity, while maintaining a fully random orientation distribution. Each mechanism contributes a component of strain. Fig. 8 illustrates the two cases.

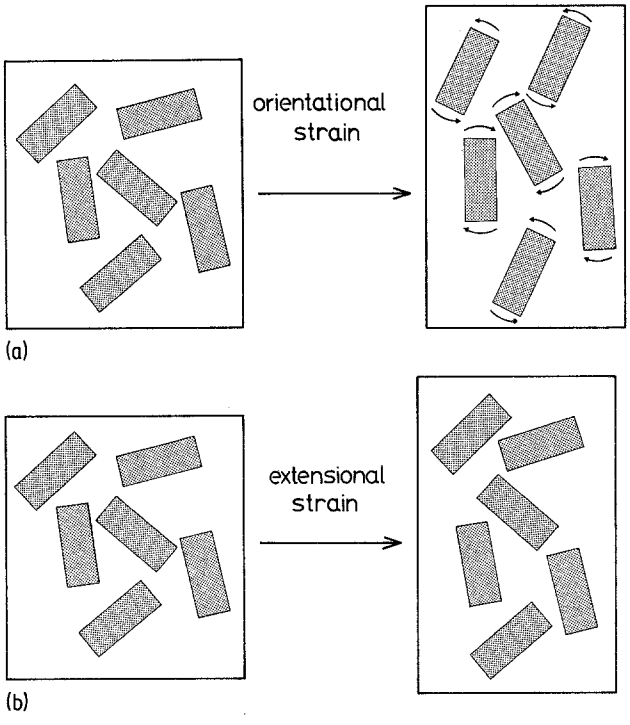

Figure 8 (a) Schematic representation of the orientational component of deformation. (b) Schematic representation of the extensional component of deformation.

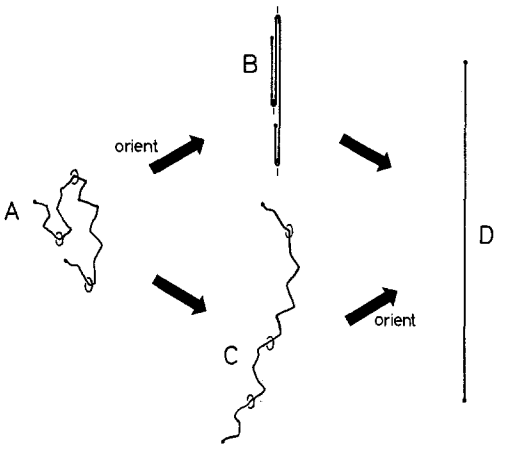

Figure 9 Two-mode strategy: the two extreme cases. A, undeformed chain; B, orientational deformation mode only; C, extensional deformation mode only; D, fully extended chain after both modes have operated.

In a real solid, of course, there must be some constraint on the movement of any structural unit: if there were none, the situation would be one of liquid-like flow. Firstly, the units will be strung together into macromolecular chains, which will restrict the relative motion of units belonging to the same chain. Secondly, steric interaction between segments of neighbouring chains will demand some degree of co-operation in the movement of adjacent units. Thirdly, the presence of cross-links – whether inter-chain covalent bonds or mechanical entanglements – will further limit the relative motion of units, most significantly by imposing a maximum attainable extension and thus preventing true liquid-like viscous flow.

These sources of constraint, and the need for a degree of co-operative unit movement which they impose, will mean that the orientational and extensional components of deformation will in practice take effect simultaneously. Nonetheless, it is instructive to consider the two limiting cases (Fig. 9). We start with a macromolecule in, for the sake of argument, a random coil configuration: it may be depicted as a random chain containing n links (denoted A). Let the individual links rotate so as to become aligned in some unique direction: this will lead to a configuration such as B, with complete orientation of all the links, but maintaining several reversals of direction. If the oriented chain is now "untwisted" about these reversal points, we obtain the fully extended chain D. Alternatively, we can do the "untwisting" first, to give the unravelled chain C: although we have produced some strain, there is no tendency to link alignment (given the reasonable assumption that links in the chain are non-polar). Subsequent link alignment again gives the fully extended chain D.

These two "limiting cases" – two routes from random coil to fully extended chain – thus illustrate the separation of the two components of strain. Stages A–B and C–D represent orientational deformation, while stages B–D and A–C are purely extensional, involving no change whatever in the orientation distribution function for the links of the chain. The response of an assemblage of anisotropic units to the applied stress acting upon each unit through its environment is not seen, therefore, as primarily a consequence of the fact that units belong to molecular chains. Rather, the role of the chain is in suppressing relative motion of individual units, so that the orientational component of strain becomes significant without extensive and rapid viscous flow occurring at the same time: thus the assemblage behaves as a solid.

5. Summary

The primary objective of this work is to understand why links of the molecular chain align much more rapidly per unit plastic strain in the glassy state than in the rubbery state. A profound difference in deformation mechanism is implied, yet in each case the structure at the limiting strain of comparatively well aligned molecules appears the same, and indeed a plastically deformed glass warmed to above its T_g is able to assert its entropic elasticity and spring back into its original shape.

We have set out to describe the behaviour of a polymer in either the rubbery or the glassy state by resolving the deformation into two components, one involving the alignment of the chain links with the tensile axis (the orientational component) and the other involving the unravelling of the chain. The latter component is not associated with alignment. The value of this artificial separation into two components arises from the association of the extensional component with longer range adjustments in the disposition of chain segments than those associated with the orientational component. Below the glass transition, where thermal activation becomes a limiting factor, one may expect the longer range component of deformation to be suppressed in relation to the orientational. It is this feature which imparts to the two-component approach the potential ability to account both for the pronounced differences in orientation–strain

relationships above and below the glass transition, and for the differing rates at which measured orientation and overall strain relax in the vicinity of T_g.

A model which can describe differences between deformation in the rubbery and glassy states qualitatively may be of interest, but if it is not able also to account for both rubbery and glassy behaviour quantitatively it will be of little real value. This is perhaps particularly important in regard to rubber elasticity, where well-established chain statistical theories have been developed in detail.

A first step in testing the two-component model – based on the approach set out above, and developed in detail in Part 2 – must be to examine its ability to predict both the stress–strain behaviour characteristic of rubbery elasticity, and the observed development of molecular orientation as a function of stress or of strain.

It is clear, that in viewing rubber as a state of matter rather than the secretion of a tree, one should look for data from as wide a range of examples of the rubbery state as possible. However, the most studied rubber is natural rubber (*cis*-polyisoprene) itself, and data on other rubbers which relate stress, strain and orientation are very rare indeed. A consequence of reviewing the stress–orientation–strain (SOS) data which do exist is the indication that to take natural rubber as the archetype of the rubbery state is perhaps misleading. The theories developed to account for the SOS behaviour of natural rubber are elegant in that they require few structure-related constants. However the existing theories only give satisfactory predictions for PMMA and non-crystalline PET, behaving as rubbers, if the structure-related constants vary with strain, as is illustrated by the $n - \lambda$ plots of Figs. 3 and 4.

The comparison of the SOS relationship by the new model with those observed experimentally is thus not straightforward, for one has to decide whether to select data for, say, natural rubber alone, or whether to accept predictions which lie generally in the range of data for different rubbers. If the model is able to give even a broad prediction of a wide range of observed rubber behaviour, then it will be worthwhile to apply it to the glassy state for further testing. However, the detailed comparisons with the rubber data which are made in Part 2 in fact reflect significantly on existing theories based on the concept of affine chains.

Appendix: The description and analysis of chain orientation

The purpose of this appendix is to review in outline the established work which relates orientation of chain segments to parameters such as strain. In doing so, the methods for description of orientation which will be used in the two subsequent papers are also introduced.

The description of orientation

A first requirement is to define some quantitative measure of orientation. In the most general case, we would consider an orthogonal set of axes fixed in the appropriate structural unit, and describe the orientation of the latter in terms of three Eulerian angles. These represent three successive rotations necessary to bring the axes into coincidence with a reference set fixed in the macroscopic specimen. Such a description of orientation is general but complicated. Fortunately, we can often introduce considerable simplification by assuming that, upon deformation, there is no tendency to alignment in a plane perpendicular to some particular direction (typically the draw direction for a fibre), i.e. that we have transverse isotropy. An associated assumption on a molecular level is that there is no tendency to alignment of any structural axes or "directors" other than those representing the backbone chain axes. It may be assumed that under uniaxial tensile stress these directors tend to align parallel to the direction of stress, so that we can equate the unique molecular axis to the "laboratory axis" corresponding to the draw direction. Such an assumption is usually applicable to non-crystalline polymers: it does not, of course, require that the molecular chain itself has cylindrical symmetry.

The uniaxial simplification allows us to describe orientation in terms of an orientation distribution function (ODF) $\rho(\phi)$, where ϕ is the angle between a director and the reference axis. We have

$$\int_0^{\pi/2} \rho(\phi) \sin\phi \, d\phi = 1 \qquad \text{(A1)}$$

The factor $\sin\phi$ arises from the "degeneracy" of ϕ: i.e. the fact that if each director can choose its direction about the axis at random, the probability of ϕ taking some particular value will be proportional to $\sin\phi$.

One method of representing $\rho(\phi)$ is to draw a three-dimensional representation surface with the radius in a direction given by ϕ corresponding to

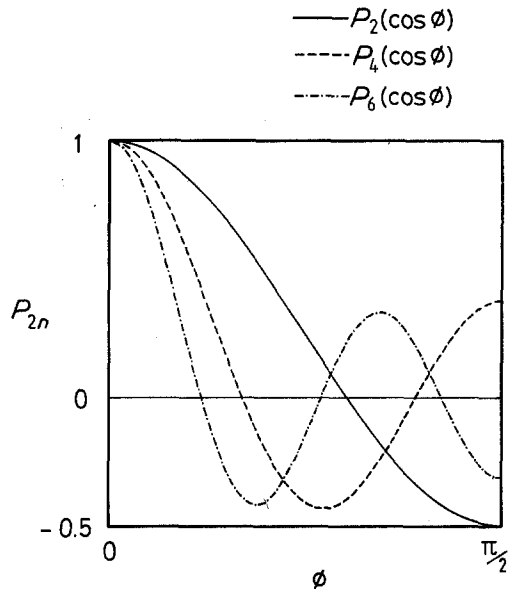

Figure 10 Spherical harmonics $P_{2n}(\cos\phi)$ against ϕ.

the magnitude of $\rho(\phi)$ in that direction. For uniaxial "fibre" symmetry such a surface would be an ellipsoid of revolution, something like a rugby ball. We could transfer the information to two dimensions by means of a stereographic projection with suitable contours, i.e. a pole figure, but a more powerful technique is to express $\rho(\phi)$ as a series of spherical harmonics, in terms of the Legendre polynomials, P_n. These have the advantage of orthogonality (that is, we can change one harmonic without necessarily changing the others), and analysing the "rugby ball" in terms of spherical harmonics is analogous to analysing a wave into its Fourier components. We require only the Legendre polynomials of even order in $\cos\phi$, and the first few are:

$$P_0(x) = 1 \tag{A2}$$

$$P_2(x) = \tfrac{1}{2}(3x^2 - 1) \tag{A3}$$

$$P_4(x) = \tfrac{1}{8}(35x^4 - 30x^2 + 3) \tag{A4}$$

$$P_6(x) = \tfrac{1}{16}(231x^6 - 315x^4 + 105x^2 - 5) \tag{A5}$$

Their relationship to ϕ is shown in Fig. 10. We will denote mean values of the even order Legendre polynomials by $\langle P_{2n}(\cos\phi)\rangle$. For a random distribution all the $\langle P_{2n}\rangle$ are zero, while for complete alignment along some unique axis all take the value 1. Higher order polynomials may be obtained by using the recurrence relation

$$P_n(x) = \frac{1}{n}[(2n-1) \times x \times P_{n-1}(x) - (n-1) \times P_{n-2}(x)] \tag{A6}$$

It can then be shown [30] that the distribution function is

$$\rho(\phi) = \sum_{n=0}^{\infty} 2(n + 1/2) \times \langle P_n(\cos\phi)\rangle \times P_n(\cos\phi) \tag{A7}$$

and that the individual polynomials are given by

$$\langle P_n(\cos\phi)\rangle = \int_0^{\pi/2} \rho(\phi) P_n(\cos\phi) \sin\phi \, d\phi \tag{A8}$$

It will be usually be sufficient for the analysis of predicted orientation or of experimental data to consider values of the low-order Legendre polynomials rather than the full orientation distribution function given by Equation A7.

The use of the $\langle P_{2n}\rangle$ has the further advantage of allowing description of successive "levels" of orientation. Suppose for example that molecules are partially oriented within some microscopic domain, and that the domains are themselves oriented with respect to some reference axis (we assume that both distributions are uniaxially symmetric). Then for the overall orientation as measured experimentally, each $\langle P_{2n}\rangle$ will be given by the product of the $\langle P_{2n}\rangle$ for the orientation of the molecules with respect to the domain axis, and the $\langle P_{2n}\rangle$ for the orientation of the domain axes themselves with respect to the reference axis.

Experimental techniques available for orientation measurement will yield the required mean values of $\cos^{2n}\phi$. The oldest, conceptually simplest, and certainly the most colourful technique is that of optical birefringence, which formed the basis of the historical development of the rubber photoelasticity theory summarized below. However, it yields only $\langle\cos^2\phi\rangle$: $\langle\cos^4\phi\rangle$ and higher even powers are accessible by other methods, with wide angle X-ray scattering (WAXS) able in principle to yield any required even power and hence any $\langle P_{2n}\rangle$. The chief techniques have been reviewed [1–5].

Affine deformation: rubbery photoelasticity

The historical starting point for orientation studies is the optical anisotropy or birefringence

of natural rubber, first analysed by Kuhn and Grün [31] using a method closely related to their treatment of chain elasticity. The theory is set out in detail by Treloar [8].

We first recall that the polarizability of a medium is defined as the induced dipole moment per unit field strength. We denote polarizability by γ for one "random link", by p for a single chain, and by B for the whole network; the subscripts 1, 2 indicate "axial" and "transverse" directions.

Kuhn and Grün show that the polarizability anisotropy for a freely jointed random chain of vector length r, comprising n links of length l, is

$$p_1 - p_2 = n(\gamma_1 - \gamma_2)\left(1 - \frac{3r/nl}{\mathscr{L}^{-1}(r/nl)}\right) \quad \text{(A9)}$$

This is the same for all chains (under affine deformation) since it depends only on the ratio r/nl. The term in the square brackets, containing the inverse Langevin function $\mathscr{L}^{-1}(x)$, varies between 0 and 1: Treloar calls this the relative chain anisotropy. It can be expanded as an infinite series in (r/nl):

$$p_1 - p_2 = n(\gamma_1 - \gamma_2)[\tfrac{3}{5}(r/nl)^2 + \tfrac{36}{175}(r/nl)^4 + \tfrac{108}{175}(r/nl)^6 + \ldots] \quad \text{(A10)}$$

Taking the first term in such an expansion is analogous to using the Gaussian approximation for chain entropy, and gives:

$$p_1 - p_2 = (3/5)n(\gamma_1 - \gamma_2)(r/nl)^2. \quad \text{(A11)}$$

For an isolated chain this will give a value of $(3/5)(\gamma_1 - \gamma_2)$, i.e. 3/5 of the anisotropy of a single link.

Kuhn and Grün then consider a Gaussian network containing N chains per unit volume, with their end-to-end vectors (r-vectors) at first distributed randomly in direction. The polarizabilities of the network, with respect to the principal axes of strain, are found by integration over all chains. The principal polarizabilities must then be converted to principal refractive indices μ_1, μ_2: in making this conversion Kuhn and Grün assume that the mean square end-to-end distance of the chains in the network is nl^2 (just as for a set of free chains) and, in effect, that the difference in refractive indices is small in comparison to their mean. They obtained the polarizability–refractive index relationship:

$$\frac{4\pi}{3}(B_1 - B_2) = \frac{6\mu_0}{(\mu_0^2 + 2)^2} \times (\mu_1 - \mu_2) \quad \text{(A12)}$$

where μ_0 is the mean refractive index, given by $\frac{1}{3}(\mu_1 + 2\mu_2)$. The orientation parameter $\langle P_2 \rangle$ is simply the difference in polarizabilities, normalized by dividing by the theoretical total polarizability if all the links in the network could be aligned:

$$\langle P_2 \rangle = (B_1 - B_2)/Nn(\gamma_1 - \gamma_2) \quad \text{(A13)}$$

so that for practical purposes, $\langle P_2 \rangle$ will be proportional to the birefringence $(\mu_1 - \mu_2)$ so long as μ_0 remains constant. Treloar calls $\langle P_2 \rangle$ the optical orientation factor: it is also sometimes termed the Hermans orientation function.

Kuhn and Grün's expression for orientation birefringence as a function of the uniaxial extension ratio λ is:

$$\mu_1 - \mu_2 = \frac{2\pi}{45} \times \frac{(\mu_0^2 + 2)^2}{\mu_0} \times N(\gamma_1 - \gamma_2)(\lambda^2 - 1/\lambda) \quad \text{(A14)}$$

or in terms of $\langle P_2 \rangle$:

$$\langle P_2 \rangle = \frac{1}{5n}(\lambda^2 - 1/\lambda) \quad \text{(A15)}$$

The limiting extension ratio under affine conditions is $n^{1/2}$, so that $\langle P_2 \rangle$ corresponding to this limit tends to 1/5 as n becomes large.

The result of Equation A14 was used by Treloar [9] in conjunction with the stress–strain relationship derived from the simple statistical theory of rubber elasticity to give a linear relationship between birefringence and true stress:

$$\mu_1 - \mu_2 = C(\sigma_1 - \sigma_2) \quad \text{(A16)}$$

where σ_1, σ_2 are the appropriate principal stresses, and the strain-independent constant C – the stress-optical coefficient – is given by

$$C = \frac{2\pi}{45kT} \times \frac{(\mu_0^2 + 2)^2}{\mu_0}(\gamma_1 - \gamma_2) \quad \text{(A17)}$$

The treatment set out above can be extended to non-Gaussian networks by taking more than one term in the expansion (Equation A10); Kuhn and Grün themselves went on to take three terms. Other workers [32, 33] follow a similar method but with slightly different assumptions: for example, Treloar [32] modifies the Kuhn–Grün model by assigning the "free chain" mean square value of r to all chains in the network (rather than using a distribution of r), which means in effect that he assigns smaller coefficients to the second and higher terms in the series expansion.

Treloar [32] also quotes an empirical closed series expansion of the relative chain anisotropy; it is accurate to better than 1% over the entire range of r/nl, and is a convenient alternative to Equation A10:

$$1 - \frac{3r/nl}{\mathscr{L}^{-1}(r/nl)} \simeq \tfrac{3}{5}(r/nl)^2 + \tfrac{1}{5}(r/nl)^4 + \tfrac{1}{5}(r/nl)^6 \quad \text{(A18)}$$

All these attempts at describing non-Gaussian behaviour lead to a $\langle P_2 \rangle$ against strain plot which exhibits a faster upward curvature than the Gaussian case, while the birefringence–true stress relationship becomes both non-linear (approaching an asymptotic limit at high stresses) and dependent on n, the number of links per chain. Such attempts are still very approximate since they consider a set of chains of equal length, for, as Treloar [8] points out, a distribution of chain lengths (i.e. of n) should be considered.

A broader view of orientational deformation

It is impossible to characterize a distribution of some quantity fully by specifying only one scalar parameter. While $\langle P_2 \rangle$ is sometimes used as a sole "order parameter" for oriented systems, the ambiguity this leaves can be illustrated by the case $\langle P_2(\cos\phi) \rangle = 0$, which can correspond either to completely random orientation, or (among other things) to a situation where $\phi = 54.736^\circ$ for all units*.

In view of this ambiguity it is perhaps unfortunate that the nature of birefringence, as the most important technique historically, has concentrated attention only on $\langle P_2(\cos\phi) \rangle$, given by the fractional birefringence $\Delta\mu/\Delta\mu_0$. Although $\langle P_2 \rangle$ is the most accessible orientation parameter both experimentally and by calculation, it gives only the first term in the ODF. The question of exactly how much we *do* know about the overall form of the ODF, when we have measured only the first one or two spherical harmonics, constitutes an interesting problem. It has been considered in detail by Nomura *et al.* [34, 35] and by Bower [36]: we may summarize the situation by saying that high order terms tend to be both small and experimentally inaccessible, but that a consideration of at least $\langle P_4 \rangle$ is highly desirable.

To obtain expressions for the orientation functions of order higher than two we employ the useful properties of spherical harmonics. Consider a network of random chains subjected to uniaxial deformation, e.g., by fibre drawing. The individual links of each chain will be uniaxially distributed about the r-vector, and we can describe their distribution by an ODF involving the usual series of spherical harmonics, $P_{2n}(\cos\psi)$. Here we use ψ to denote the angle between a link and the r-vector. However, we also have a further "level" of orientation: the r-vectors will themselves be uniaxially distributed about the draw direction, with a distribution function involving a second series of spherical harmonics, $P_{2n}(\cos\Phi)$, where Φ is the angle between an r-vector and the draw direction. According to our introductory consideration of spherical harmonics, we should now be able to find the overall orientation parameters by simply multiplying those for the two underlying distributions:

$$\langle P_{2n}(\cos\phi) \rangle = \langle P_{2n}(\cos\psi) \rangle \times \langle P_{2n}(\cos\Phi) \rangle \quad \text{(A19)}$$

(where as usual ϕ is the angle between an individual link and the macroscopic draw direction).

In practice the situation is not quite this simple, because any average involving ψ will itself be a function of our other variable Φ. We have therefore to perform an integration (actually, we are convoluting the two distributions):

$$\langle P_{2n}(\cos\phi) \rangle = \int_0^\pi \langle P_{2n}(\cos\psi) \rangle \times P_{2n}(\cos\Phi) \times D(\Phi)\,\mathrm{d}\Phi \quad \text{(A20)}$$

Here $D(\Phi)\mathrm{d}\Phi$ represents the fraction of r-vectors which lie at angles in the range Φ to $\Phi + \mathrm{d}\Phi$. To carry out the integration we must first express $\langle P_{2n}(\cos\psi) \rangle$ in terms of Φ; for this purpose it is useful to make the abbreviations

$$t = r/ml \quad \text{(A21)}$$

$$\beta = \mathscr{L}^{-1}(t) \quad \text{(A22)}$$

where r and l have their usual meaning, and to

*This is not as unlikely as it sounds. Many experiments do not measure the orientation of the main chain directly, but make use of the dipole moment associated with some sidegroup. Imagine a situation where the main chains were completely aligned, but had sidegroups at some fixed angle to the backbone axis. If this angle were near 54.7° the parameter $\langle P_2(\cos\phi) \rangle$ could remain near zero, notwithstanding the main chain alignment.

avoid confusion the number of links per chain is denoted by m. Φ and t are related by:

$$t^2 = \frac{\lambda^2}{m[\cos^2\Phi + \lambda^3(1-\cos^2\Phi)]} \quad \text{(A23)}$$

Then, following Roe and Krigbaum [37] and Nobbs and Bower [38]:

$$\begin{aligned}
\langle P_0(\cos\psi)\rangle &= 1 \\
\langle P_2(\cos\psi)\rangle &= 1 - 3t/\beta \\
\langle P_4(\cos\psi)\rangle &= 1 - 10t/\beta + 35/\beta^2 - 15t/\beta^3 \\
\langle P_6(\cos\psi)\rangle &= 1 - 21t/\beta + 189/\beta^2 - 1260t/\beta^3 \\
&\quad + 3465/\beta^4 - 10395t/\beta^5 \quad \text{(A24)}
\end{aligned}$$

Secondly, we need an expression for $D(\Phi)\mathrm{d}\Phi$. It is convenient to express this too in terms of $\cos\Phi$, so that, following Kuhn and Grün [31]:

$$D(\cos\Phi)\,\mathrm{d}(\cos\Phi) = \frac{\lambda^3\,\mathrm{d}(\cos\Phi)}{2[\cos^2\Phi + \lambda^3(1-\cos^2\Phi)]} \quad \text{(A25)}$$

Using Equations A23–A25 and our usual expressions A2 *et seq.* for $P_{2n}(x)$ we can tackle the integral A20, expressed in terms of $\cos\Phi$ as:

$$\langle P_{2n}(\cos\phi)\rangle = \int_{-1}^{1} \langle P_{2n}(\cos\psi)\rangle \times P_{2n}(\cos\Phi) \times D(\cos\Phi)\,\mathrm{d}(\cos\Phi) \quad \text{(A26)}$$

With the aid of a computer we can evaluate this integral for any $\langle P_{2n}(\cos\phi)\rangle$. Analytical solutions are possible, though laborious: Roe and Krigbaum [37] calculate $\langle P_2\rangle$, $\langle P_4\rangle$ and $\langle P_6\rangle$ for Treloar's modified (non-Gaussian) Kuhn–Grün model, using three terms of the expansion A10. Nobbs and Bower [38] show that better results are obtained using the alternative expansion A18: Fig. 11 (solid lines) shows the behaviour of $\langle P_2\rangle$ and $\langle P_4\rangle$ for a 25-link chain, using the Nobbs and Bower equations. The latter are reproduced in Fig. 12. Several characteristic features are to be noted:

(i) the gradient of $\langle P_2\rangle$ against λ increases with strain: orientation develops slowly at first because the end-to-end length of the chain is very much less than its contour length. There is "plenty of slack in the chain". It is therefore possible to extend the chain greatly, by changing its conformation, without bringing in much alignment of the links. Later, however, as we "take up the slack", the random links become more closely aligned with the end-to-end vectors, and further deformation is accompanied by a more pronounced increase in $\langle P_2\rangle$.

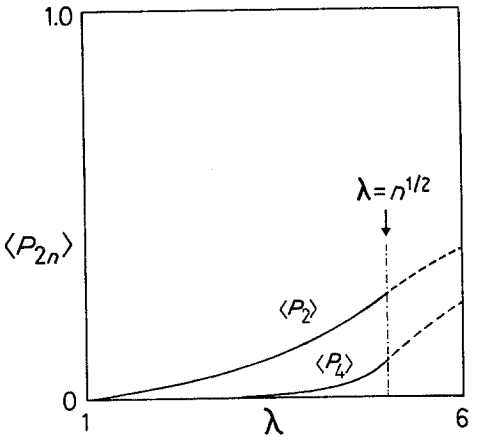

Figure 11 Orientation against extension ratio for a network with 25 links per chain (after Nobbs and Bower [38]). Dashed lines represent Nobbs and Bowers "mathematical device" to go beyond the affine limit $\lambda = n^{1/2}$.

(ii) At all strains up to $\lambda = n^{1/2}$, $\langle P_4\rangle$ is very small compared to $\langle P_2\rangle$, although the gradient again increases with λ.

(iii) The "upturn" in both parameters is associated with limiting network extensibility: it will clearly come into play at lower strains for lower values of n, and at any given strain the $\langle P_{2n}\rangle$ values will therefore increase as n decreases.

All this of course limited to strains below $\lambda = n^{1/2}$, the maximum possible extension ratio in the affine deformation scheme. Nobbs and Bower [38], following Purvis and Bower [10], endeavour to extend the description of network orientation beyond this limit (presumably for application to highly oriented drawn fibres) by making two assumptions which although strictly incompatible, are useful "simply as a mathematical device". The assumptions are:

(a) Any chain which becomes fully extended subsequently rotates as a rigid rod, with an orientation changing like that of the line joining two points in an affinely deforming continuum, i.e. pseudo-affinely;

(b) The end-to-end vectors of other chains continue both to rotate and to extend according to the affine scheme.

These assumptions lead to the continuations of the $\langle P_2\rangle$ and $\langle P_4\rangle$ plots shown as dashed lines in Fig. 11. The relevant equations are given in Fig. 12.

(a)

$$\langle P_2 \rangle = \frac{1}{5n}\left[\lambda^2 - \frac{1}{\lambda}\right] + \frac{1}{25n^2}\left[\lambda^4 + \frac{\lambda}{3} - \frac{4}{3\lambda^2}\right] + \frac{1}{35n^3}\left[\lambda^6 + \frac{3\lambda^3}{5} - \frac{8}{5\lambda^3}\right]$$

$$\langle P_4 \rangle = \frac{-\lambda^5}{360n}\left[\frac{8\lambda^6 + 33\lambda^3 - 6}{3\lambda^6(\lambda^3 - 1)} - \frac{35}{(\lambda^3 - 1)^2}\left[1 - \frac{\tan^{-1}(\lambda^3 - 1)^{\frac{1}{2}}}{(\lambda^3 - 1)^{\frac{1}{2}}}\right]\right] + \frac{94}{1125n^2}\left[\lambda^4 - 2\lambda + \frac{1}{\lambda^2}\right] - \frac{151}{1575n^3}\left[\lambda^6 - \frac{4\lambda^3}{5} - \frac{7}{5} + \frac{6}{5\lambda^3}\right] + \frac{112}{2025n^4}\left[\lambda^8 - \frac{2\lambda^5}{7} - \frac{37\lambda^2}{35} - \frac{36}{35\lambda} + \frac{48}{35\lambda^4}\right] + \frac{7}{275n^5}\left[\lambda^{10} - \frac{5\lambda^4}{7} - \frac{22\lambda}{21} - \frac{16}{21\lambda^2} + \frac{32}{21\lambda^5}\right] + \frac{84}{2925n^6}\left[\lambda^{12} + \frac{2\lambda^9}{11} - \frac{5\lambda^6}{11} - \frac{200\lambda^3}{231} - \frac{32}{33} - \frac{128}{231\lambda^3} + \frac{128}{77\lambda^6}\right] + \frac{7}{1125n^7}\left[\lambda^{14} + \frac{4\lambda^{11}}{13} - \frac{37\lambda^8}{143} - \frac{290\lambda^5}{429} - \frac{2720\lambda^2}{3003} - \frac{2624}{3003\lambda} - \frac{384}{1001\lambda^4} + \frac{256}{143\lambda^7}\right] + \frac{7}{3825n^8}\left[\lambda^{16} + \frac{2\lambda^{13}}{5} - \frac{7\lambda^{10}}{65} - \frac{28\lambda^7}{55} - \frac{112\lambda^4}{143} - \frac{128\lambda}{143} - \frac{128}{165\lambda^2} - \frac{512}{2145\lambda^5} + \frac{4096}{2145\lambda^8}\right]$$

(b)

$$\langle P_2 \rangle = 1 - \frac{128}{175x^{\frac{1}{2}}}$$

$$\langle P_4 \rangle = 1 - \frac{0.9022}{x^{\frac{1}{2}}} \qquad (x^2 = \lambda^2/n)$$

Figure 12 Orientation functions for affine deformation, after Nobbs and Bower [38]. n = number of links in the chain, λ = extension ratio. (a) Treloar's closed series approximation. (b) Extension above an extension ratio $n^{1/2}$.

The pseudo-affine deformation scheme

In the pseudo-affine deformation scheme the rod-like units rotate in a similar way to that required in affine deformation, but are unable to change in length. The mathematical relationship between the affine and pseudo-affine schemes can be clearly seen from the integral in Equation A26. Suppose that a chain becomes fully extended. All the terms $\langle P_{2n}(\cos\psi)\rangle$ then become unity, since $\psi = 0$ for all links. For such chains the integral then describes simply the orientation of the r-vectors, which are rotating without further change of length in accordance with the constraints imposed by the affinely deforming body in which they are "embedded" – i.e. they are deforming pseudo-affinely. This is not surprising, since the pseudo-affine deformation scheme, notwithstanding its origins in crystallite orientation, is in fact only describing the orientation of a set of lines drawn in an affinely deforming continuum. The pseudo-affine orientation functions can therefore be expressed by modifying Equation A26 to give:

$$\langle P_2(\cos\phi)\rangle = \frac{1}{2}\left[\frac{2+k^2}{1-k^2} - \frac{3k\cos^{-1}k}{(1-k^2)^{3/2}}\right]$$

$$\langle P_4(\cos\phi)\rangle = \frac{1}{8}\left\{\frac{35}{(1-k^2)^2}\left[1+\frac{k^2}{2} - \frac{3k\cos^{-1}k}{2(1-k^2)^{1/2}}\right] - \frac{30}{1-k^2}\left[1 - \frac{k\cos^{-1}k}{(1-k^2)^{1/2}}\right] + 3\right\}$$

Figure 13 Orientation functions for the pseudo-affine deformation scheme, after Ward [2], with $k = \lambda^{-3/2}$.

$$\langle P_{2n}(\cos\phi)\rangle = \int_{-1}^{1} P_{2n}(\cos\Phi) \times D(\cos\Phi)\,\mathrm{d}(\cos\Phi) \qquad \text{(A27)}$$

where ϕ and Φ are now equivalent.

The analytic expressions for $\langle P_2\rangle$ and $\langle P_4\rangle$ are given in Fig. 13, and the behaviour plotted in Fig. 14. Several contrasts with the affine scheme are apparent:

(i) There are no adjustable parameters: the values of $\langle P_{2n}(\cos\phi)\rangle$ depend solely on strain (and not, for example, upon n).

(ii) The absolute magnitudes of $\langle P_2\rangle$ and $\langle P_4\rangle$ are, at a given strain, much greater than their affine counterparts.

(iii) The magnitude of $\langle P_4\rangle$ is comparable with that of $\langle P_2\rangle$, coming within a factor of 2 for $\lambda \gtrsim 2$.

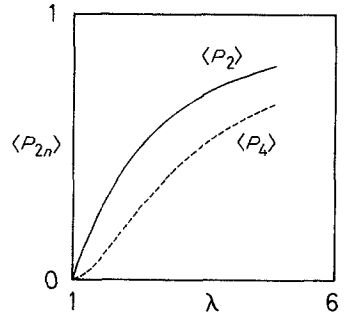

Figure 14 Orientation functions $\langle P_2(\cos\phi)\rangle$ and $\langle P_4(\cos\phi)\rangle$ for pseudo-affine deformation, as functions of extension ratio.

Non-uniaxial geometries

Although the spherical harmonics $\langle P_{2n}\rangle$ are strictly applicable only to uniaxial geometries, it is useful to evaluate their analogues in other geometries. This may be achieved by modifying the distribution function $D(\Phi)\mathrm{d}\Phi$ (i.e. the "pseudo-affine" part of the integral). The general expression is given by Sasaguri *et al.* [39]: one particularly useful special case to consider is the plane strain geometry (Fig. 15). Here we have a sheet specimen compressed between two polished dies, such that the die length is long compared to the die width. The constraint imposed by the undeformed material on either side of the deformed area prevents motion parallel to the length of the dies [40]. Thus in the notation of Fig. 15 the strain in the y direction is, ideally, zero. For the two specific planes of interest

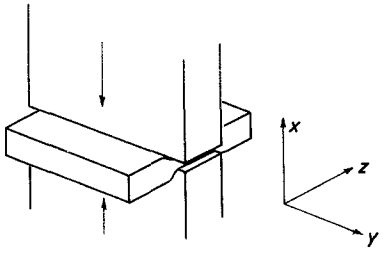

Figure 15 The plane strain compression geometry: strain in the y direction is zero, and the extension ratio is usually taken to be greater than 1, i.e.

$$\lambda = \lambda_z = 1/\lambda_x.$$

Birefringence may be measured under load in the z–x plane, and after unloading in the z–x or (more conveniently) the y–z plane.

the general expression for $D(\cos\Phi)$ simplifies to:

$$D(\cos\Phi)\,d(\cos\Phi) = \frac{\lambda^3 d(\cos\Phi)}{2\pi(\cos^2\Phi + \lambda^2\sin^2\Phi)^{-3/2}}$$

(y–z plane) (A28)

$$D(\cos\Phi)\,d(\cos\Phi) = \frac{\lambda^3 d(\cos\Phi)}{2\pi(\cos^2\Phi + \lambda^4\sin^2\Phi)^{-3/2}}$$

(z–x plane) (A29)

By suitable substitution in Equation A26 or A27 we obtain the "plane strain analogues" of the $\langle P_{2n}(\cos\phi)\rangle$. The y–z expression is equivalent to the f_{zy} of Pick *et al.* [6].

For plane strain deformation, the fractional birefringence and the "$\langle P_2\rangle$ analogue" f_{zy} as measured by WAXS will no longer be equal. This is because all chain segments will contribute to the measured birefringence in any given plane, whereas in WAXS the specimen is rotated about an axis (for f_{zy} the x-axis), so that the scattering vector always lies in the plane normal to that axis. Only those segments which lie in the plane of the scattering vector will contribute to the measured WAXS orientation parameters. However, Pick *et al.* show that in the case of pseudo-affine deformation the difference between fractional birefringence and f_{zy} is always small (up to about 5%).

References

1. I. M. WARD (ed.), "Structure and Properties of Oriented Polymers" (Applied Science Publishers, London, 1975).
2. *Idem, J. Polym. Sci., Polym. Symp.* 58 (1977) 1.
3. G. L. WILKES, *Adv. Polym. Sci.* 8 (1971) 91.
4. *Idem, J. Macromol. Sci., Rev. Macromol. Chem.* 10 (1974) 149.
5. M. MAY, *J. Polym. Sci., Polym. Symp.* 58 (1977) 23.
6. M. PICK, R. LOVELL and A. H. WINDLE, *Polymer* 21 (1980) 1017.
7. L. R. G. TRELOAR, *Trans. Faraday Soc.* 40 (1944) 59.
8. *Idem,* "The Physics of Rubber Elasticity", 3rd edn, (Oxford University Press, London, 1975).
9. *Idem, Trans. Faraday Soc.* 43 (1947) 277, 284.
10. J. PURVIS and D. I. BOWER, *J. Polym. Sci., Polym. Phys. Ed.* 14 (1976) 1461.
11. A. CUNNINGHAM, I. M. WARD, H. A. WILLIS and V. ZICHY, *Polymer* 15 (1974) 749.
12. J. H. NOBBS, D. I. BOWER, I. M. WARD and D. PATTERSON, *ibid.* 15 (1974) 287.
13. J. H. NOBBS, D. I. BOWER and I. M. WARD, *ibid.* 17 (1976) 25.
14. D. J. BROWN and G. R. MITCHELL, *J. Polym. Sci., Polym. Lett. Ed.* 21 (1983) 341.
15. D. J. BROWN, PhD thesis, University of Cambridge (1982).
16. I. M. WARD, "Mechanical Properties of Solid Polymers" (Wiley, New York and London, 1971).
17. O. KRATKY, *Kolloid Z.* 64 (1933) 213.
18. J. F. RUDD and E. F. GURNEE, *J. Appl. Phys.* 28 (1957) 1096.
19. S. RAHA and P. B. BOWDEN, *Polymer* 13 (1972) 174.
20. N. KAHAR, R. A. DUCKETT and I. M. WARD, *ibid.* 19 (1978) 136.
21. A. H. WINDLE, in "Developments in Oriented Polymers – 1" edited by I. M. Ward (Applied Science Publishers, London, 1982).
22. T. E. BRADY and G. S. Y. YEH, *J. Polym. Sci., Part B* 10 (1972) 731.
23. *Idem, J. Macromol. Sci. Phys.* B7 (1973) 243.
24. P. R. PINNOCK and I. M. WARD, *Trans. Faraday Soc.* 62 (1966) 1308.
25. F. RIETSCH, R. A. DUCKETT and I. M. WARD, *Polymer* 20 (1979) 1133.
26. A. KELLER, *J. Polym. Sci., Polym. Symp.* 58 (1977) 395.
27. A. CIFERRI and I. M. WARD (eds.) "Ultra-High Modulus Polymers" (Applied Science Publishers, London, 1979).
28. F. C. FRANK, *Proc. Roy. Soc. London* A319 (1970) 127.
29. C. C. HSIAO and S. R. MOGHE, *J. Macromol. Sci. Phys.* B5 (1971) 263.
30. V. J. MCBRIERTY and I. M. WARD, *Brit. J. Appl. Phys.* 1 (1968) 1529.
31. W. KUHN and F. GRÜN, *Kolloid Z.* 101 (1942) 248.
32. L. R. G. TRELOAR, *Trans. Faraday Soc.* 50 (1954) 881.
33. K. J. SMITH and D. PUETT, *J. Appl. Phys.* 37 (1966) 346.
34. S. NOMURA, H. KAWAI, I. KIMURA and M. KAGIYAMA, *J. Polym. Sci., Part A2* 8 (1970) 383.
35. *Idem, ibid.* 9 (1971) 407.
36. D. I. BOWER, *J. Polym. Sci., Polym. Phys. Ed.* 19 (1981) 93.
37. R. J. ROE and W. R. KRIGBAUM, *J. Appl. Phys.* 35 (1964) 2215.
38. J. H. NOBBS and D. I. BOWER, *Polymer* 19 (1978) 1100.
39. K. SASAGURI, S. HOSHINO and R. S. STEIN, *J. Appl. Phys.* 35 (1964) 47.
40. J. G. WILLIAMS and H. FORD, *J. Mech. Eng. Sci.* 6 (1964) 405.
41. G. R. DOBSON and M. GORDON, *Trans. Inst. Rubber Ind.* 40 (1964) T262.

Received 7 September
and accepted 22 September 1983